Polymers from Sugars and Cyclic Anhydrides: Ring Opening Copolymerization of a D-Xylose Anhydrosugar Oxetane

*Thomas M. McGuire,[a] Ella F. Clark[a] and Antoine Buchard[a]**

Centre for Sustainable and Circular Technologies, Department of Chemistry, University of Bath, Claverton Down BA2 7AY Bath, UK.

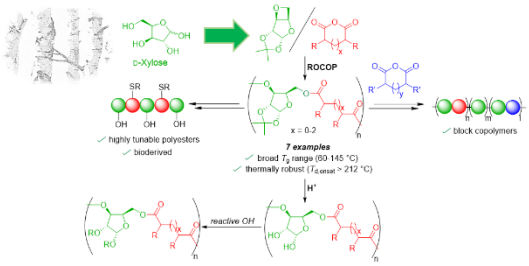

Figure for Table of Contents use only

ABSTRACT A D-xylose 3,5-anhydrosugar derivative has been used as an oxetane co-monomer in the ring-opening copolymerization (ROCOP) with cyclic anhydrides, to form a family of seven novel sugar-derived polyesters, with up to 100% renewable content. ROCOP proceeds with high alternating selectivity to form AB-type co-polymers which are thermally robust ($T_{d,onset}$ > 212 °C) and exhibit a broad range of glass-transition temperatures (T_g 60–145 °C). These polyesters are amenable to further post-polymerization functionalization. The hydroxy group of the sugar moiety

can be unveiled then functionalized further, *e.g.* phosphorylated. The internal alkene of some of the anhydride moieties can also be subject to thiol-ene reactions. Combining those orthogonal strategies affords AB co-polyesters with alternating functional substituents. By exploiting the living character of the ROCOP process, block co-polymers have also been synthesized through sequential co-monomer addition experiments.

INTRODUCTION

Environmental concerns surrounding the extensive use of fossil-fuel derived plastics is driving research into renewable feedstocks for polymer materials, towards a more sustainable plastics economy. One sustainable alternative to crude-oil feedstock is lignocellulosic biomass, which may be obtained from agricultural waste. Hemicellulose comprises 20-30 wt% of lignocellulosic biomass and is the second most abundant biopolymer on earth. Owing to the relatively short chain length of hemicelluloses (<200 degrees of polymerization), it may be readily processed, for instance by acid hydrolysis, to xylose and other monosaccharides (*e.g.* mannose). As such, xylose has been identified by our group, and others, as a candidate for carbohydrate-based polymer synthesis. More generally, carbohydrates represent a renewable resource with significant potential in polymer synthesis.[1-5] The low cost of starting materials and the presence of multiple hydroxy groups significantly broaden the scope of prospective functionality and applications, while polymers which maintain the cyclic core of sugars form materials have also been shown to lead to desirable thermal properties such as high glass transition temperatures.[6-10]

Besides transesterification[3] and acyclic diene metathesis[11-12] polymerization techniques, recent reports on the incorporation of unmodified sugar-cores within polymer chains have been most frequently involving ROP of functionalized sugar derivatives,[4] including cyclic carbonates,[6-10, 13] phosphoesters[14] and thiocarbonates.[15] ROP is a powerful living polymerization method, able

to control efficiently degree of polymerization and to produce copolymers, but the synthesis of sugar-based cyclic monomers is generally labor intensive and variation of the polymer structure typically requires chemical modification of the monomer and is thus non-trivial.[4, 16] Conversely, the ring opening copolymerization (ROCOP) of cyclic ethers with various monomers (*e.g.* cyclic anhydrides, CO_2 and CS_2) to form alternating (AB-type) polyesters,[17-18] polycarbonates[19] and polythiocarbonates[20] can easily produce multiple polymer types and functionalities by simple variation of the co-monomers. ROCOP is also a living polymerization technique, allowing control of molar masses via a chain transfer agent, as well as formation of block-copolymers through sequential monomer addition. Numerous highly active ROCOP catalysts have been developed to date, including metal complexes based on salen[21-24] (Al(III), Co(II/III, Cr(III), Ni(II)) salan (Cr(III)), Robinson macrocycles[25-27] (Zn(II), Mg(II)), trisphenolate (Fe(III)), beta diiminate (Zn(II)) and porphyrin (Al(III), Cr(III), Co(III)) ligands. Compared to the ROCOP of cyclic ethers with heterocumulenes like CS_2 and CO_2, ROCOP of cyclic ethers with cyclic anhydrides is particularly attractive owing to the wealth of known compounds of both types. This double synthetic manifold potentially gives access to a wide array of structurally diverse polyesters. Accordingly, in conjunction with advances in catalysis, such flexibility allows material properties (*e.g.* thermal and chemical stability), to be targeted for particular applications, even from a single cyclic ether monomer.

Typically, epoxides are applied in ROCOP owing to their relatively high ring strain, and reports of ROCOP with oxetanes are rare. Generally, oxetanes are more challenging to prepare than epoxides and exhibit increased stability as a result of unfavorable kinetics of opening in conjunction with comparatively low ring strain.[28-29] While oxetane/CO_2 cycloaddition into cyclic carbonates and ROCOP into polycarbonates has been known for some time,[30-38] examples of

oxetane and cyclic anhydride ROCOP remain limited to a couple of examples. The first report of oxetane/anhydride ROCOP was made by Endo and co-workers who used bulky titanium bisphenolate complexes as catalysts to form polyesters of moderate molar mass ($M_{n,SEC}$ up to 6300 g mol^{-1}; $Đ_M$ = 1.18–1.60),[39] albeit with significant ether link formation (34–54%). A few years later, Nishikubo and co-workers described an onium salt initiated oxetane/anhydride ROCOP which occurred in the absence of a metal-based co-catalyst and which resulted in highly regular alternating copolymers ($M_{n,SEC}$ up to 11100 g mol^{-1} ; $Đ_M$ = 1.13–1.43).[40]

Our group,[12, 41] amongst many others,[9, 42-45] have identified D-xylose as a promising sustainable feedstock for polymer synthesis, owing to its low cost, abundance and low toxicity, as well as its potential for pre- or post-polymerization functionalization, due to multiple hydroxy groups. From 1,2-isopropylidene-D-xylofuranose, a 3,5-anhydrosugar derivative **1**, can be readily obtained, which features an oxetane ring fused to the xylofuranose core. Comparatively, **1** exhibits markedly less strain than that of a typical epoxide (*e.g.* cyclohexene oxide (CHO)) as indicated by DFT ring strain calculations (Scheme S1, isodesmic opening with acetic anhydride ΔΔH (**1**) = –25.5 kcal mol^{-1}; *vs* ΔΔH (CHO) = –36.1 kcal mol^{-1}). While this oxetane monomer has been previously homopolymerized in a regioregular fashion, both by cationic,[44-45] and more recently, by anionic methods,[41] to the best of our knowledge no reports have been made on its ROCOP with any co-monomer. More generally, the ROCOP of a functionalizable oxetane derived from renewable feedstock has never been reported.

Herein, we described the ROCOP of **1** with various monocyclic, bicyclic and tricyclic anhydrides to form seven novel polyesters. Sequential co-monomer addition experiments enabled the synthesis of block-copolymers. In addition, by taking advantage of the pendant OH groups of the xylofuranose and where appropriate, thiol-ene chemistry, the polyesters were shown to be

amenable to multiple orthogonal post-polymerization functionalization. All these novel materials were fully characterized by NMR spectroscopy, size-exclusion chromatography (SEC), differential scanning calorimetry (DSC), thermogravimetric analysis (TGA) and wide-angle X-ray scattering (WAXS) analysis.

RESULTS AND DISCUSSION

ROCOP of oxetane 1 with phthalic anhydride. Oxetane **1** was readily prepared in three steps from D-xylose as previously reported (Scheme 1). Protection of the 1,2-positions of D-xylose was achieved by selective ketal formation under acidic conditions, followed by tosylation to form tosyl ester, **2**. Subsequent cyclisation, facilitated by an excess of KOMe, and distillation of the oxetane over CaH_2, yielded **1** in 74% yield. We note that the synthesis of **1** was scalable and reactions were performed with up to 20 g of xylose, without requiring column chromatography.

Scheme 1. Synthesis of 1 from D-xylose

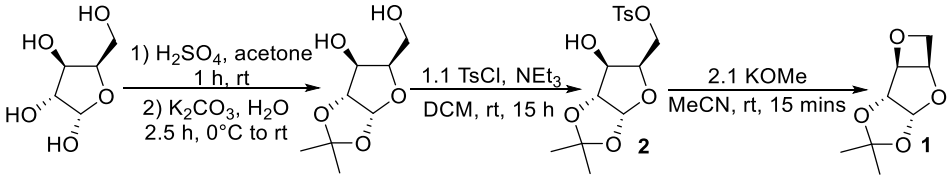

The copolymerization of **1** with phthalic anhydride, **PA**, was first investigated with *rac* 1,2-Cyclohexanediamino-N,N'-bis(3,5-di-*t*-butylsalicylidene)chromium(III), **CrSalen**. **CrSalen**, was chosen because of its well-known versatility as an anhydride/epoxide and CO_2/oxetane ROCOP catalyst,[17-18, 46-48] even if its application in oxetane/anhydride ROCOP remains unexplored. Polymerizations were initially trialed at $[\mathbf{1}]_0$:$[\mathbf{PA}]_0$:$[\mathbf{CrSalen}]_0$:$[PPNCl]_0$ loadings of 100:100:1:1, 60 °C and $[\mathbf{1}]_0$ = 2 mol L^{-1} in toluene (Table 1, entry 1). The appearance of new resonances in ^1H NMR spectroscopy at 5.48 ppm suggested the formation of ester linkages, later

confirmed by ^{1}H-^{13}C 2D NMR spectroscopy, however, the reaction proved sluggish, with only 9% conversion of **1** after 53 h.

The temperature was then increased to 100 °C and solvent changed from PhMe to σ-dichlorobenzene to reduce solvent reflux. This led to improved reactivity, although solidification of the reaction mixture prior to completion of the reaction limited monomer conversion to 85% after 41 h (Table 1, entry 2). To mitigate solidification, [**1**]$_0$ was decreased to 1.34 mol L^{-1}, resulting in 97% conversion of the oxetane after 89 h (Table 1, entry 3). At [**1**]$_0$:[**PA**]$_0$:[**CrSalen**]$_0$:[PPNCl]$_0$ loadings of 200:200:1:1, molar masses ($M_{n,SEC}$) of up to 14000 g mol $^{-1}$ and narrow dispersities ($Đ_M$) of 1.24–1.27 could be obtained, as measured by SEC (against narrow polystyrene standards). Rates could be dramatically improved by performing the reaction in absence of solvent, however, solidification of the reaction mixutre limited monomer conversion and $M_{n,SEC}$ (Table 1, entry 4). Control experiments with only **CrSalen** (without PPNCl) and only PPNCl (without **CrSalen**) gave no conversion of **1** (Table 1, entries 5 and 6, respectively). Under identical conditions, bimetallic Zn macrocyclic complex, **LZn$_2$Ph$_2$**, and heterobimetallic Zn/Mg macrocyclic complex, **LZnMg(C$_6$F$_5$)$_2$**, which have been developed by Williams and co-workers and have shown high activity in epoxide/anhydride and epoxide/CO_2 ROCOP,[26-27, 49-51] proved catalytically inactive (Table 1, entries 7 and 8, respectively). These data could suggest that more Lewis acidic complexes are required for efficient ROCOP of **1**. However, analogous **AlSalen** (Al((III)) and **CoSalen** (Co(II)) complexes, in combination with PPNCl, showed limited success in converting **1** into polymer (Table 1, entries 9 and 10, respectively). In addition, spectroscopic analysis of the product from reactions using **AlSalen** and **CoSalen** revealed a less regular microstructure than that produced by **CrSalen** (Figure S115), demonstrating less selectivity in alternating ROCOP (*vide infra*). The use of KO^{t}Bu and 18-crown-6, which proved successful in

the anionic homopolymerisation of **1** in bulk at 120 °C,[41] also gave only minimal conversion of **1** both in solution and in the absence of solvent (Table 1, entries 11 and 12, respectively).

Table 1. Initial conditions and catalytic systems screened for the ROCOP of **1** and **PA**

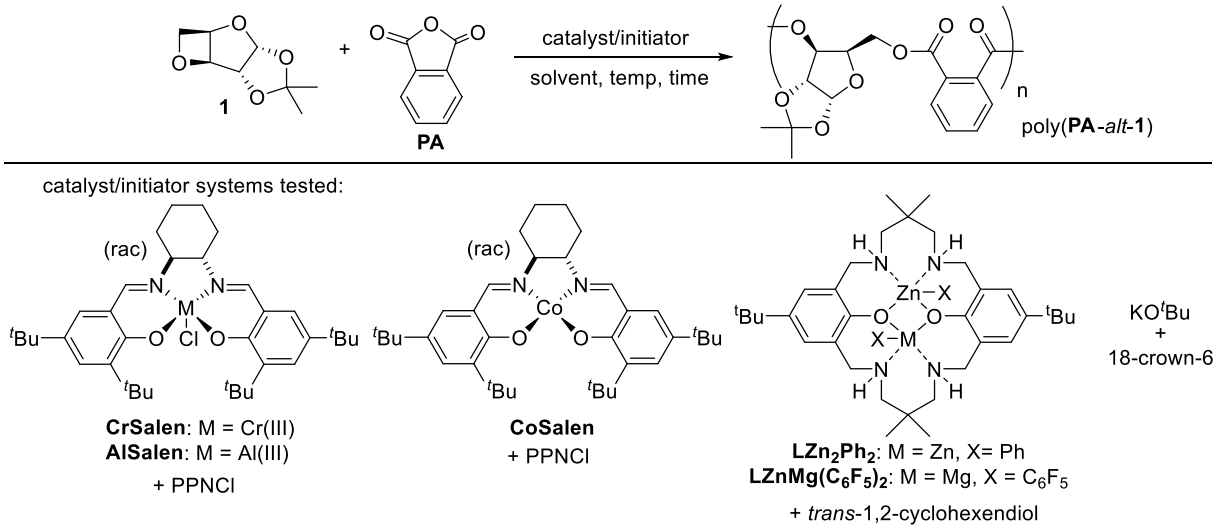

Entry[a]	Catalyst	[**1**]$_0$:[**PA**]$_0$:[cat]$_0$:[I]$_0$	Temp (°C)	Time (h)	Conv.[b] (selectivity)[c]	TOF[d] (h^{-1})	$M_{n,SEC}$ ($Đ_M$)[e]
1[f]	**CrSalen**	100:100:1:1	60	53	9% (-)	-	-
2[g]	**CrSalen**	200:200:1:1	100	41 [15]	85%[h] (>95%) [27%]	4.1 [3.6]	9900 (1.26)
3	**CrSalen**	200:200:1:1	100	89 [17]	97% (>95%) [28% (>95%)]	2.2 [3.2]	14000 (1.27)
4[i]	**CrSalen**	200:200:1:1	100	20	57% (>95%)	4.3	6600 (1.20)
5	**CrSalen**	200:200:1:0	100	20 [93]	7% (-) [51% (>95%)]	-	- [4000 (1.34)]
6	**PPNCl**	200:200:0:1	100	20 [93]	6% (-) [18% (95%)]	-	- [<1000]
7[j]	**LZn$_2$Ph$_2$**	200:200:1:4	100	20 [93]	0 %(-) [3% (-)]	-	-
8[j]	**LZnMg(C$_6$F$_5$)$_2$**	200:200:1:4	100	24	0% (-)	-	-
9	**AlSalen**	200:200:1:1	100	20 [93]	3% (-) [11% (83%)]	-	- [1300 (1.42)]
10	**CoSalen**	200:200:1:1	100	20 [93]	5% (-) [28% (84%)]	-	- [<1000]

11[k]	KO^{t}Bu/ 18-crown-6	200:200:1:1	100	69	5%	-	-
12[i,k]	KO^{t}Bu/ 18-crown-6	200:200:1:1	100	20	0%	-	-
13	**CrSalen**	200:0:1:1	100	20 [90]	1 %(-) 3% (-)	-	-

[a] Reactions carried out at $[\mathbf{1}]_0$ = 1.34 mol L^{-1} in σ-dichlorobenzene with I = PPNCl unless otherwise stated. [b] Conversion of **1** determined by ^{1}H NMR spectroscopy by relative integration of anomeric protons in **1** ($CDCl_3$, δ = 6.26 ppm (d, J = 3.7 Hz)) and poly(**PA**-*alt*-**1**) ($CDCl_3$, δ = 5.95 ppm (d, J = 3.6 Hz)). [c] Selectivity of ester *vs* ether links determined by ^{1}H NMR spectroscopy using the relative integration of anomeric ester environments ($CDCl_3$, δ = 5.95 ppm (1H, d, J = 3.6 Hz)). *vs* methylene ether environments ($CDCl_3$, δ = 3.72 – 3.56 (2H, m)). [d] TOF = (moles of **1** consumed) × (moles of catalyst)$^{-1}$ × (time of reaction)$^{-1}$; values in square brackets taken from reaction times and conversions in square brackets. [e] M_n in g mol^{-1}, calculated by SEC relative to polystyrene standards in THF eluent; $Đ_M = M_w/M_n$. [f] $[\mathbf{1}]_0$ = 2.0 mol L^{-1}, solvent = PhMe. [g] $[\mathbf{1}]_0$ = 2.0 mol L^{-1}. [h] Polymerization quenched by cooling over ice after stirring stopped. [i] Reaction carried out neat ($[\mathbf{1}]_0$ = 3.13 mol L^{-1} assuming **1** density = 1.00 g mol^{-1}). [j] I = *trans*-1,2-cyclohexendiol. [k] I = KO^{t}Bu; cat = 18-crown-6.

^{1}H-^{13}C{^{1}H} HMBC NMR spectra demonstrated that ROCOP catalyzed by **CrSalen** proceeded selectively by opening of **1** across the oxetane moiety, as indicated by exclusive correlation of the carbonyl resonance of phthalic moiety with the ***c*** and ***e*** environments of the xylofuranose component (Figure 1b). ^{1}H NMR spectroscopy of isolated samples of polymers revealed that relative integration of the aromatic resonances accounted for the expected number of protons (four) compared with the sugar moiety (Figure 1a). Moreover, only traces of ether linkages (<5%) were observed in the ^{1}H NMR spectrum (between 3.25 – 3.75 ppm). Collectively these results suggest high selectivity of the ROCOP process towards alternating AB copolyesters, poly(**PA**-*alt*-**1**). Control experiments performed in the absence of **PA** resulted in only 1% conversion of **1** after 20 h at $[\mathbf{1}]_0$:$[\mathbf{CrSalen}]_0$:$[PPNCl]_0$ loadings of 200:1:1 at 100 °C, demonstrating that **CrSalen** indeed does not catalyze the ROP of **1** within the timeframe, stoichiometries and temperatures of ROCOP employed here (Table 1, entry 13).

In addition, at 100 °C with [**1**]$_0$:[**PA**]$_0$:[**CrSalen**]$_0$:[PPNCl]$_0$ loadings of 200:200:1:1, the rates of consumption of both **PA** and **1** were very similar which is strongly indicative of *AB*-type polymer microstructure (Figure S118). The alternating nature of poly(**PA**-*alt*-**1**) was further supported by MALDI-time-of-flight (MALDI-ToF) mass spectrometry analysis, which detected polymeric series with repeat units of 320 g mol^{-1}, consistent with an alternating **PA 1** polymer sequence (Figure 1c, Figure S156 and Table S1).

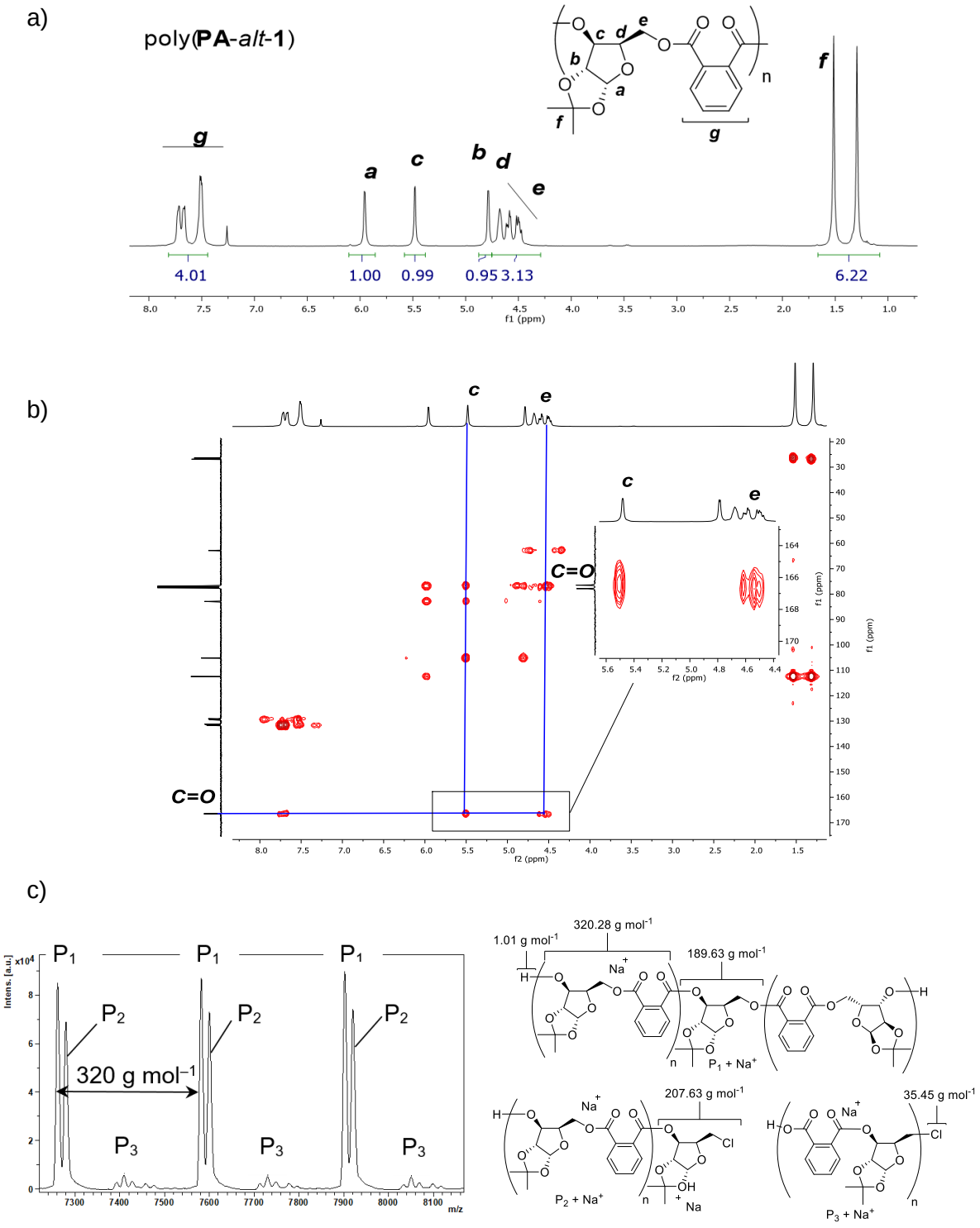

Figure 1. a) ^{1}H and b) ^{1}H-^{13}C HMBC NMR spectra ($CDCl_3$) of isolated poly(**PA**-*alt*-**1**). c) Zoomed in MALDI-ToF spectrum showing detected series. The primary and secondary series are assigned

as linear polymer species with 1,2-O-isopropylidene-α-D-xylofuranose and OH (P_1) or Cl (P_2) chain ends. The minor series P_3 is assigned as a linear polymer species featuring chloride and carboxylic acid chain ends. All series were detected as Na^+ adducts.

^{1}H and ^{13}C{^{1}H} NMR spectroscopy further showed that poly(**PA**-*alt*-**1**) was also highly regioregular (Figures S5 and S6), suggesting propagation occurs regioselectively, presumably *via* opening of **1** to expose the more acidic secondary alkoxide. Inspection of the carbonyl region of the ^{13}C{^{1}H} NMR spectrum revealed the presence of only two resonances for the **PA** moiety, strongly indicative of head-to-tail (HT) or tail-to-head linkages (TH), formed by the consistent, regioselective opening of **1** by the propagating carboxylate growing polymer, into either a secondary or primary alkoxide, respectively. On the other hand, this observation is incompatible with head-to-head (HH) and tail-to-tail (TT) linkages, as these would occur alternatively and result in four resonances (with each arrangement contributing two) (see Figure S116 for more details on how HH, TH, HH and TT links could form). Lastly, ^{1}H COSY NMR spectroscopy showed no coupling between the ***b*** and ***c*** environments which is suggestive of a HT microstructure (Figure S7).

SEC analysis at intermediate conversions showed a bimodal distribution (Figure S157), likely as a result of initiation by chloride anions as well as diprotic impurities in **1** and **PA,** as typically observed in ROCOP. MALDI-ToF mass spectrometry corroborated this as three polymer series were detected as sodium adducts (P1, P2 and P3, Figure 1c, Figures S156 and Table S1). Series P2 and P3 both result from the initiation of the polymerization by chloride anions and are end-capped with hydroxy and carboxylate groups, respectively. Series P1, on the other hand, is end-capped on both termini by hydroxy secondary group, and results from the initiation of the polymerization by 1,2-O-ispropylidene-α- D-xylofuranose diol, which is likely being formed by

hydrolysis of **1**. The absence of terminal primary hydroxyl groups was confirmed by phosphorous end group titration experiments:[52] ^{1}H, ^{31}P and ^{1}H-^{31}P HMBC NMR spectroscopy revealed the presence of >95% secondary alcohol end groups (Figure S185 and 186).

Preliminary reaction monitoring by ^{1}H NMR spectroscopy over three days with **CrSalen**/PPNCl at [**1**]$_0$:[**PA**]$_0$:[**CrSalen**]$_0$:[PPNCl]$_0$ loadings of 200:200:1:1 potentially indicate first-order kinetics (k_{obs}**1** = 0.0267 h^{-1}, k_{obs}**PA** = 0.0222 h^{-1}) with respect to [**1**] and [**PA**] (Figure S118), although a more in depth kinetic analysis would be required for accurate determination of rate constants and orders in substrates. Similarly, TOF values were lower in the reaction of **1** and **PA** than for other known **CrSalen** catalysed epoxide/anhydride ROCOPs (TOF = 75.8 h^{-1}, temperature = 110 °C, [**PA**]$_0$ = 2.5 mol L^{-1}, [**PA**]$_0$:[Cyclohexene Oxide]$_0$:[**CrSalen**]$_0$:[PPNCl]$_0$ = 250:250:1:1).[53] Regardless of this slow reaction rate, some degree of polymerization control was observed, with M_n increasing linearly with conversion of [**1**]$_0$ (Figure S119) as typically observed in living polymerizations. In addition, the polymerization remained controlled throughout the reaction with $Đ_M$ values between 1.2–1.3. However, despite the living nature of the ROCOP, $M_{n,SEC}$ values were considerably lower than theoretical ones ($M_{n,theo}$) (*e.g.* for entry 3 of Table 1, $M_{n,theo}$ = 57000 g mol^{-1} *vs* $M_{n,SEC}$ = 14000 g mol^{-1}), likely due to the presence of residual protic impurities as indicated in the MALDI-ToF mass spectrum and bimodal SEC chromatograms (Figure 1 and Figure S157). This suggests that improved control over the M_n of the co-polymer could be obtained by removing residual impurities.

ROCOP of oxetane 1 with selected mono-, di- and tricyclic anhydrides. The protocol was next extended to a range of cyclic anhydride co-monomers. For 5-membered monocyclic anhydrides, succinic anhydride (**SA**), maleic anhydride (**MA**) and citraconic anhydride (**CA**),

conversions of **1** were poor and only oligomers were detected by SEC (Table 2, entries 1–3). For **MA** and **CA**, at 100 °C broad resonances were detected at 1.00 – 3.50 ppm, suggesting the occurrence of cross-linking of the anhydride's alkene moeity.[47] However, a reaction performed at 60 °C with **CA,** resulted in no conversion of either co-monomer after 1 week .

Table 2. ROCOP of **1** with various anhydrides

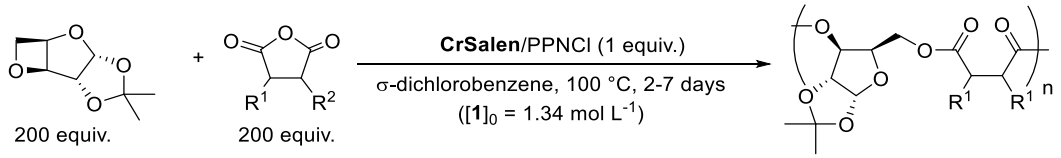

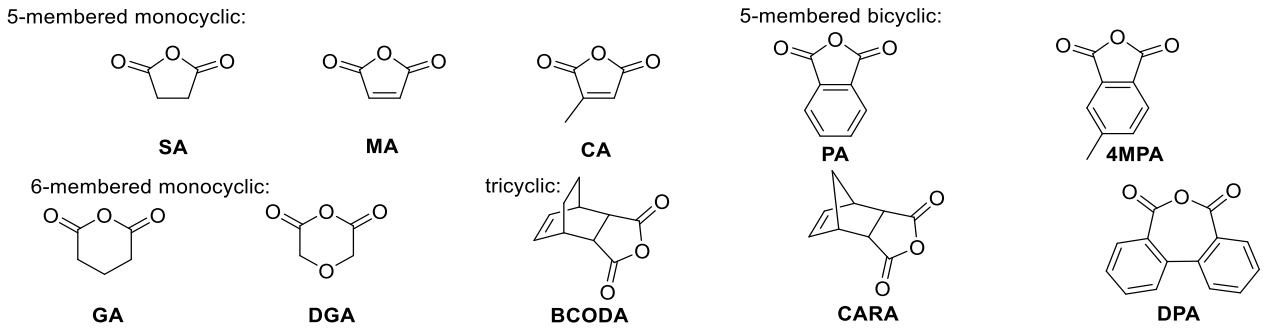

Entry	Anhydride	Time (h)	Conv. (%)[a]	Select. (%)[b]	TOF (h^{-1})[c]	$M_{n,theo}$ [d]	$M_{n,SEC}$[e]	$Đ_M$[f]	T_g (°C)[g]	$T_{d,onset}$ (°C)
1	**SA**	41	29[h]	-	1-	-	<1000	-	-	-
2	**CA**	41	0 [0][i]	-	-	-	-	-	-	-
3	**MA**	41	0	-	-	-	-	-	-	-
4	**PA**	89	97	>95	2.2	64000	14000	1.24	145	241
5	**4MPA**	55	95	>95	3.5	66900	12300	1.27	138	235
6	**GA**	131	97	>95	1.5	57300	7200	1.40	60[j]	280
7	**DGA**	143	95	>95	1.3	57700	6300	1.59	80	269
8	**BCODA**	61	83	>95	2.7	70000	4200	1.23	131	263
9	**CARA**	143	84	>95	1.2	67000	12000	1.35	141	212
10	**DPA**	41	99	>95	4.9	79300	10500	1.29	129	296

[a] Conversion of **1** determined by relative integration of anomeric protons in **1** ($CDCl_3$, δ = 6.26 ppm (d, J = 3.7 Hz)) and polymer ($CDCl_3$, δ = 6.01–5.44 ppm), reaction quenched when stirring stopped. [b] Selectivity of ester *vs* ether links determined by ^{1}H NMR spectroscopy using the relative integration of anomeric ester environments ($CDCl_3$, δ = 6.01–5.44 ppm, 1H) *vs* methylene ether environments ($CDCl_3$, δ = 3.72 – 3.56, 2H (m)). [c] (moles of **1** consumed) × (moles of catalyst)$^{-1}$ × (time of reaction)$^{-1}$ values in square brackets taken from reaction times and conversions in square brackets. [d] Calculated as M_r(Cl)+ ((M_r(**1**)+M_r(anhydride)) × [**1**]$_0$/ [PPNCl]$_0$ × %conv./100). [e] Calculated by SEC relative to polystyrene standards in THF eluent. [f] $Đ_M = M_w/M_n$. [g] Values taken from second heating cycle. [h] conversion identical to that after 21 h. [i] reaction carried out at 60 °C. [j] crystallinity observed by WAXs (*vide infra*).

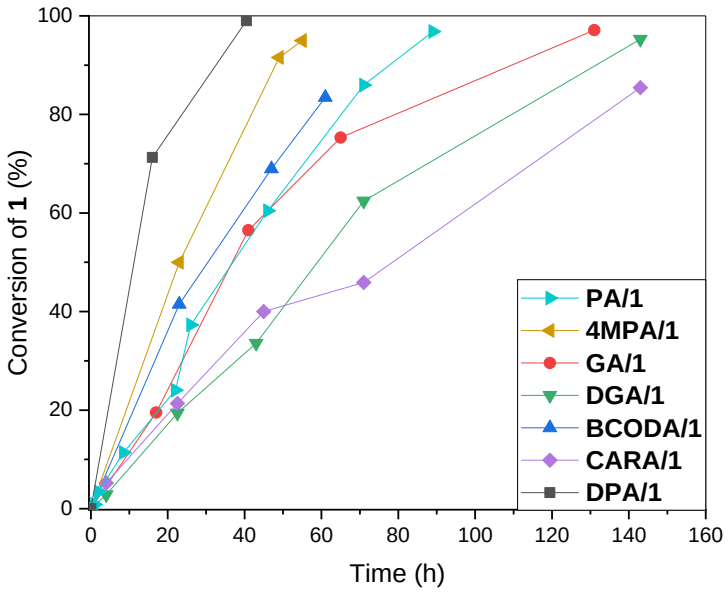

Figure 2. Conversion of **1** (determined by ^{1}H NMR spectroscopy) in ROCOP with **PA** (cyan), **4MPA** (orange), **GA** (red), **DGA** (green), **BCODA** (blue), **CARA** (purple) and **DPA** (dark grey) at 100 °C with [**1**]$_0$:[anhydride]$_0$:[**CrSalen**]$_0$:[PPNCl]$_0$ loadings of 200:200:1:1. [1]$_0$ = 1.34 mol L^{-1} in σ-dichlorobenzene.

For all other substrates tested, ROCOP proceeded as intended (Table 2, entries 4–10, Figure 2). High selectivity for ROCOP was observed for each anhydride (>95%) in line with the limited catalytic activity of **CrSalen** for the ROP of **1**. In the case of 4-methylphthalic anhydride, **4MPA**, conversions, turn over frequency (TOF) and $M_{n,SEC}$ values were comparable to those observed with **PA** (Table 2, entries 4 and 5, respectively), indicating the remote Me group does not interfere with the ROCOP process. Similarly, conversions, TOF and $M_{n,SEC}$ values were approximately the same for glutaric anhydride, **GA**, and diglycolic anhydride, **DGA** (Table 2, entries 6 and 7, respectively). For the tricyclic anhydrides, *endo*-Bicyclo[2.2.2]oct-5-ene-2,3-dicarboxylic anhydride**, BCODA,** and carbic anhydride, **CARA**, conversions were similar, however, TOF was lower for the latter, with $M_{n,SEC}$ values higher (Table 3, entries 8 and 9,

respectively). Finally, for diphenyl anhydride, **DPA**, faster and up to quantitative conversion of **1** were observed, consistent with the increased reactivity brought by the added ring strain of the 7-membered anhydride (Table 2, entry 10). While TOF values were higher for **DPA** as compared with all the other anhydrides tested, $M_{n,SEC}$ values were comparable to that obtained with **PA** and **4MPA**. As commonly observed in the field,[17, 54-56] for all anhydrides tested, the $M_{n,SEC}$ values were significantly lower than theoretical molar masses ($M_{n,theo}$), likely as a result of protic impurities present in the reaction mixtures. This was substantiated by SEC data which showed that polymer distributions were generally either bimodal or with small shoulders (Figures S159–164), indicative of several concurrent initiation processes as previously discussed (Figure 1). However, efforts to increase the M_n values in **PA**/**1** ROCOP through sublimation of **PA**, as well as successive distillations of **1** and reaction with NaH/MeI prior to distillation in order to quench diprotic impurities,[57] failed to yield higher molar mass polymers.

For poly(**4MPA**-*alt*-**1**), poly(**GA**-*alt*-**1**) and poly(**DGA**-*alt*-**1**), ^{1}H and ^{13}C{^{1}H} NMR spectroscopy suggested that opening of **1** proceeded regioselectively, likely *via* the less basic secondary propagating alkoxide, as each polymer had the expected number of resonances present in the corresponding spectra. With poly(**BCODA**-*alt*-**1**) and poly(**CARA**-*alt*-**1**), the alkene function remained intact, but significant epimerization of the protons α to the ester link was observed, probably due to the presence of alkoxide species in solution combined with high reaction temperatures and long reaction times.[17, 58-60] This leads to a change in stereochemistry of the bicyclic unit, promoting formation of the more thermodynamically stable *trans* isomer. (poly(**BCODA**-*alt*-**1**) *cis*/*trans* = 39:61 and poly(**CARA**-*alt*-**1**) 50:50). Finally, the complexity of the ^{1}H and ^{13}C{^{1}H} NMR spectra of poly(**DPA**-*alt*-**1**) suggested that in this case, ROCOP proceeded with no regioselective preference.

Thermal properties of copolymers. The thermal properties of the polyesters were next investigated. Thermogravimetric analysis (TGA) revealed that the polymers had onset of degradation temperatures ($T_{d,onset}$) between 212 °C and 295 °C (Table 2, Figures S134–140; measured under argon atmosphere). No obvious general trend between co-monomer and thermal stability was observed, however, incorporation of an oxygen atom in poly(**DGA**-*alt*-**1**) led to an approximate 20 °C decrease in $T_{d,onset}$ as compared with poly(**GA**-*alt*-**1**).

DSC (Figures S134–140) and WAXS (Figures S149–155) revealed that all the novel polymers were amorphous, except poly(**GA**-*alt*-**1**). WAXS for poly(**GA**-*alt*-**1**) showed some sharp peaks (Figure S152) while multiple crystalline domains were observed in the first heating cycle by DSC (Figure S137) with the second heating cycle only displaying a small endothermic peak ($T_m \approx$ 81 °C). This indicates that poly(**GA**-*alt*-**1**) crystallises slowly from the melt. Semicrystalline polymers comprise some of the most widely used materials in the world (*e.g.* polyethylene, polypropylene), and such properties are attractive, especially when the materials may be entirely bio-derived, as is the case with poly(**GA**-*alt*-**1**). Poly(**GA**-*alt*-1) is one of the few known semi-crystalline polyesters synthesised by ROCOP.[17, 61]

Poly(**GA**-*alt*-**1**) and poly(**DGA**-*alt*-**1**) have the lowest T_g values of 60 °C and 80 °C, respectively, consistent with the flexibility brought by the aliphatic anhydride monomer (*vs* aromatic and alicyclic anhydrides) (Table 2, entries 6 and 7, respectively). The higher T_g of poly(**DGA**-*alt*-**1**) compared to poly(**GA**-*alt*-**1**) is likely a result of O atom lone pairs increasing polarity of the chain and acting as secondary H-bond acceptor site (in addition to the carbonyl), strengthening interchain-forces and thereby decreasing chain mobility. Similar differences between the two substrates have been noted previously, with polymers derived from **DGA** typically exhibiting increased T_gs.[62]

The more rigid polyesters, namely poly(**PA**-*alt*-**1**), poly(**4MPA**-*alt*-**1**), poly(**DPA**-*alt*-**1**), poly(**BCODA**-*alt*-**1**) and poly(**CARA**-*alt*-**1**), have T_g values ranging from 129 to 145 °C (Table 2, entries 4 ,5 and 8–10). Given their high $T_{d,onset}$s, the aforementioned polymers still possess a broad processing window ($T_{d,onset} - T_g \geq 71$ °C), contrasting with previously reported sugar-based polycarbonates.[10, 13, 63] These high T_g values make the polymers attractive for applications in thermally active environments, and competive with other known high-T_g aliphatic and semi-aromatic polyesters, which are generally formed through ROCOP of bicyclic epoxides and tricyclic anhydides (with reported T_g < 184 °C).[17, 64] It should be noted that Kleij and co-workers have reported T_g values of up to 243 °C,[65] however the molecule was close to oligomeric (DP = 7, $M_{n,SEC}$ = 2200, $Đ_M$ = 1.36) and the relative low thermal stability observed ($T_{d10\%}$ = 268 °C) may limit processing and potential applications.

Poly(**PA**-*alt*-**1**) have the highest T_g of all the polymers isolated (145 °C, Table 2, entry 4). This observation contrasts with earlier reports in which tricyclic-anhydride-derived polyesters exhibited higher T_g values than bicyclic-anhydride-derived counterparts.[17, 48, 58, 64] Compared with the other high T_g polyesters formed in this study, poly(**PA**-*alt*-**1**) is distinctively regioregular. In turn, this may faciliate more efficient packing in poly(**PA**-*alt*-**1**) thereby increasing the T_g of the polymer. However, with poly(**PA**-*alt*-**1**) having the highest M_n of all isolated polymers, it is also not possible at this stage to fully delinate the impact of molar mass on T_g. Nevertheless, it is anticipated that if improved control of regio and stereoregularity of poly(**DPA**-*alt*-**1**), poly(**BCODA**-*alt*-**1**) and poly(**CARA**-*alt*-**1**) could be achieved, higher T_g values would likely be obtained.

Post-polymerization modifications: acetal deprotection and tandem functionalization. In contrast with other known high-T_g polyesters, polymers derived from **1** offer a handle for post-polymerization functionalization that is not reliant on alkene modification. To that effect, deprotection of the acetal groups of the xylose component of the polymers was next attempted under acidic conditions (Table 3). Reactions were carried out at 0 °C to minimize hydrolytic degradation of the acid-labile ester linkages. Conversions were monitored by ^{1}H NMR spectroscopy (Figure S126), and polymer degradation evaluated through SEC analysis (Figure 3, Figures S127–133 and S165–171). While it is possible that deprotection may incur significant changes in the hydrodynamic volume of the polymers, changes in $M_{n,sec}$ values after deprotection were assumed to broadly reflect chain scission.

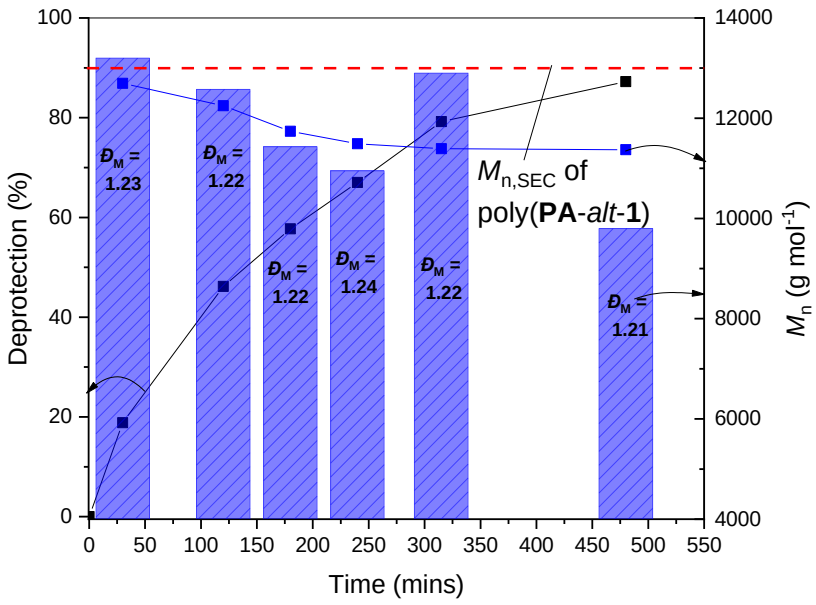

Figure 3. Deprotection (black), $M_{n,SEC}$ (bar) and $M_{n,theo}$ (blue) for acid hydrolysis of poly(**PA**-*alt*-**1**) at 0 °C. The dashed red line indicates the $M_{n,SEC}$ value of the poly(**PA**-*alt*-**1**) sample used for acetal removal. Conversion determined by ^{1}H NMR spectroscopy (DMSO-d_6) by relative

integration of the methyl groups of the isopropylidene moiety (δ = 1.42 ppm, 6H) and the aromatic resonances of the phthalic resonances (δ = 7.89 – 7.50 ppm, 4H).

The extent of hydrolytic degradation of the polymers could be correlated with the nature of the anhydride co-monomer (Figure 4). Polyesters with high glass transition temperature (made with bulkier bicyclic and tricyclic anhydrides) were generally found to be more stable to acidic conditions (Table 3, entries 1,2 and 5–7, and Figures S127, S128 and S131–133). This may be attributed to the increased steric hindrance of the polymer chain decreasing the rate of ester hydrolysis in solution. In the solid state, the relative bulk of these anhydrides also contributes to limit the free volume of the polymer, thereby decreasing segmental motion and increasing their respective T_g. Conversely, the more sterically-exposed poly(**GA**-*alt*-**1**) and poly(**DGA**-*alt*-**1**) degraded significantly upon deprotection (Table 3, entries 3 and 4, respectively and Figures S129–130), especially the latter, which, with acid-labile ether and ester linkages present in the main polymer chain, had degraded down to oligomers in 8 h (Table 3, entry 4).

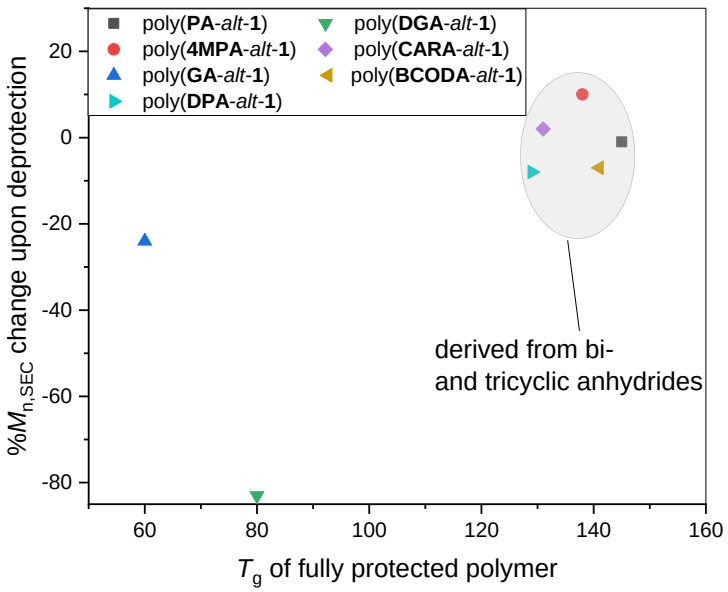

Figure 4. T_g of fully protected polymer *vs* % $M_{n,SEC}$ change upon 1,2-acetal deprotection. $M_{n,SEC}$ of protected polymers between 4000-14000 g mol^{-1}. $M_{n,SEC}$ of deprotected polymers between 1000-14000 g mol^{-1}.

Table 3. Deprotection of polyesters

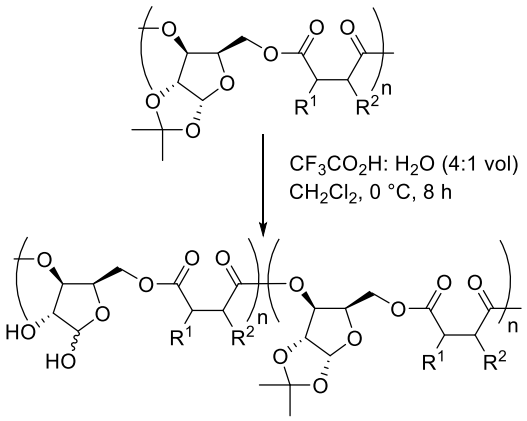

Entry	Polymer	Conv. (%)[a]	$M_{n,SEC}$ ($Đ_M$) [b]	Molar mass change[c]	T_g [ΔT_g] (°C)[d]	$T_{d,onset}$ [$\Delta T_{d,onset}$] (°C)[e]
1	**PA**-*alt*-**1**	81	12900 (1.22)[f]	–1%	135 [–10]	174 [–67]
2	**4MPA**-*alt*-**1**	79	13500 (1.51)	+10%	109 [–29]	160 [–75]
3	**GA**-*alt*-**1**	85	5500 (1.22)[f]	–24%	42 [–18]	187 [–93]
4	**DGA**-*alt*-**1**	72	1100 (1.16)	–83%	-	-
5	**BCODA**-*alt*-**1**	80	4300 (1.28)	+2%	139 [+8]	163 [–100]
6	**CARA**-*alt*-**1**	80	11200 (1.65)	–7%	148 [+7]	164 [–48]
7	**DPA**-*alt*-**1**	75	9700 (1.31)	–8%	139 [+10]	145 [–51]]

Reactions performed at 0 °C in CH_2Cl_2 at $[CF_3CO_2H]_0$ = 7.5 mol L^{-1} for 8 h unless otherwise stated. [a] Determined by ^1H NMR spectroscopy by relative integration of anomeric (d^6-DMSO, δ = 6.01–5.44 ppm) and acetal protons (d^6-DMSO, δ = 1.50–1.15 ppm). [b] Calculated by SEC relative to polystyrene standards in THF eluent, $Đ_M = M_w/M_n$. [c] 100 – (100 × M_n of deprotected polymer/$M_{n,SEC}$ of acetylated polymer). [d] Values taken from 2nd heating cycle, $\Delta T_g = \Delta T_g$ (protected) – ΔT_g (deprotected). [e] $\Delta T_{d,onset} = \Delta T_{d,onset}$ (protected) – $\Delta T_{d,onset}$ (deprotected). [f] Time = 6 h.

The SEC chromatograms of poly(**PA**-*alt*-**1**), poly(**4MPA**-*alt*-**1**) and poly(**CARA**-*alt*-**1**) also showed broadening of their respective $Đ_M$s with slight tailing towards high molar masses (Figures S165, 166 and 169, respectively). WAXS analysis of poly(**4MPA**-*alt*-**1**) corroborated the SEC data (Figure S150), with increased scattering observed at lower Q values, collectively

suggesting the presence of larger (*i.e.* cross-linked or aggregated) species. However, for poly(**BCODA**-*alt*-**1**) and poly(**DPA**-*alt*-**1**), deprotection did not induce significant changes in the scattering patterns (Figures S154 –155, S170, S171).

The effects on the thermal properties of deprotection were studied in detail with poly(**PA**-*alt*-**1**) (Table 3, entry 1, Figure 4). Exposure of 32% of the hydroxy groups led to a sharp decrease in $T_{d,onset}$ (241 °C *vs* 178 °C), which levelled off at higher percentages of deprotection (81% deprotected poly(**PA**-*alt*-**1**), $T_{d,onset}$ = 172 °C, Figure S141). Simultaneously, the T_g was found to decrease linearly with increasing percentages of deprotection, although to a much lesser extent, with 81% deprotected poly(**PA**-*alt*-**1**) exhibiting a T_g of 138 °C (compared to 145 °C for the fully protected analogue, Figure S141).

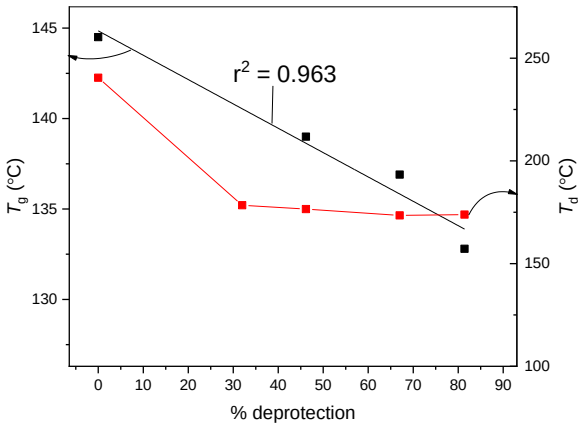

Figure 5. T_g (black) and $T_{d,onset}$ (red) *vs* % deprotection for poly(**PA**-*alt*-**1**). $M_{n,SEC}$ of deprotected poly(**PA**-*alt*-**1**) between 9000–13000 g mol^{-1}.

Similar trends in thermal stability were observed for each of the other deprotected polyesters, with $T_{d,onset}$ values decreasing to 145 – 187 °C for hydroxy-exposure levels between 75 – 85 % (Table 3, Figure S142–146). However, the effect of acid-catalyzed acetal deprotection on T_g values depended on the microstructure of the polymers. For 79% deprotected poly(**4MPA**-*alt*-

1) and 85% deprotected poly(**GA**-*alt*-**1**) the T_g's decreased by 29 °C and 18 °C (Table 3, entries 2 and 3 and Figure S142 and 143, respectively), whereas for polymers derived from tricyclic anhydrides, *i.e.*, 75% deprotected poly(**DPA**-*alt*-**1**), 80% deprotected poly(**CARA**-*alt*-**1**) and 80% deprotected poly(**BCODA**-*alt*-**1**), their respective T_g's increased by 10 °C, 8 °C and 7 °C as compared with the analogous fully acetalized polyesters (Table 3 entries 5–7, Figure S144–146). Whilst no T_m's were observed for the deprotected polymers by DSC, WAXS analysis revealed that 43% deprotected poly(**DGA**-*alt*-**1**) ($M_{n,SEC}$ = 1600, $Đ_M$ = 1.41) was crystalline (Figure S152). This suggests that either the presence of OH groups have induced crystallinity or that crystallization has been facilitated by reduced molar masses. No crystallinity was observed for any of other polymers with exposed hydroxy groups.

As a proof of concept, to assess whether the hydroxy groups in the partially deprotected polyesters were amenable to functionalization, phosphorylation of 15% deprotected poly(**PA**-*alt*-**1**) was attempted with chlorodiphenylphosphine in the presence of triethylamine and 4-dimethylaminopyridine. ^{1}H, ^{1}H-^{31}P HMBC and DOSY NMR spectroscopy (Figures S181, 183 and 184, respectively) confirmed the incorporation of the P moiety within the polymer chains while ^{31}P NMR spectroscopy revealed the phosphorous had oxidized during functionalization (Figure S182), likely as result of the presence of residual moisture in the poly(**PA**-*alt*-**1**) sample. No T_g or T_m were detected for phosphorylated poly(**PA**-*alt*-**1**) by DSC.

To demonstrate that **1** could also be applied to form AB co-polyesters with alternating functional substituents, a tandem alkene modification/acetal-deprotection strategy was employed (Table 4).[66]

Table 4. Tandem alkene modification/acetal deprotection strategy.

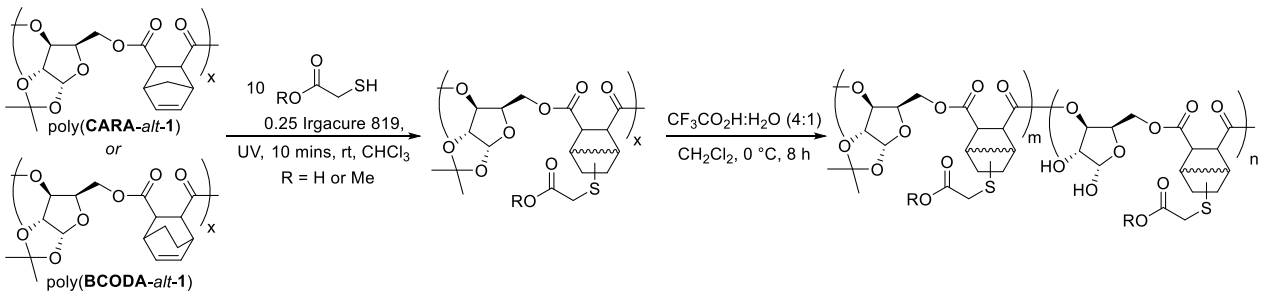

Entry	Polymer	R	$M_{n,SEC}$ original polymer ($Đ_M$) [a]	$M_{n,SEC}$ post thiol-ene functionalisation ($Đ_M$) [a]	$M_{n,SEC}$ post acetal deprotection ($Đ_M$) [a]	*m:n* [b]
1	**CARA**-*alt*-**1**	H	8200 (1.38)	2900 (1.51)	-	--
2	**BCODA**-*alt*-**1**	H	6600 (1.31)	2200 (1.20)	-	82:18
3	**CARA**-*alt*-**1**	Me	8200 (1.38)	8200 (1.60)	3600 (1.35)[c]	9:91
4	**BCODA**-*alt*-**1**	Me	6600 (1.31)	5400 (1.21)	5500 (1.75)	33:67

Thiol-ene reactions performed at room temperature in $CHCl_3$ with $[C{=}C]_0$:$[RSH]_0$:$[Irgacure819]_0$ 1:10:0.25. $[C{=}C]_0$ = 0.15 mol L^{-1}. Acetal hydrolysis reaction performed at 0 °C in CH_2Cl_2 at $[CF_3CO_2H]_0$ = 7.5 mol L^{-1} for 8 h unless otherwise stated. [a]Calculated by SEC relative to polystyrene standards in THF eluent, $Đ_M = M_w/M_n$. [c] 100 – (100 × M_n of deprotected polymer/$M_{n,SEC}$ of acetylated polymer). [b]Determined by ^{1}H NMR spectroscopy by relative integration of anomeric protons in protected (d^6-DMSO, δ = 6.00–5.78 ppm) and deprotected polymer (d^6-DMSO, δ = 5.74–5.22 ppm).[c] 10 h deprotection.

Poly(**BCODA**-*alt*-**1**) and poly(**CARA**-*alt*-**1**) were reacted with thioglycolic acid in the presence of UV-initiator Irgacure® 819 at room temperature (Table 4, entries 1 and 2). After ten minutes of UV-exposure (λ = 365 nm), ^{1}H NMR spectroscopy indicated quantitative conversion of the alkene whilst, as expected, the acetal remained intact (Figure S75). SEC analysis revealed the resulting species to still be polymeric, albeit with reduced molar masses. The acid-functionalized polymers were also found to be soluble in polar organic solvents (DMF, THF, CH_2Cl_2, $CHCl_3$, MeOH) suggesting substantial cross-linking or aggregation had not occurred. No T_g was detected by DSC. Next, the acid-functionalized polymers were subject to acetal

deprotection. However, above 16% of deprotection, the polymers precipitated from the reaction media and even at lower levels of acetal deprotection, the polymers were found to be insoluble in the available SEC eluents (THF and DMF), preventing molar mass analysis. Accordingly, we investigated the deprotection of an ester-modified poly(**CARA**-*alt*-**1**) and poly(**BCODA**-*alt*-**1**) (Table 4, entry 3). Deprotection proceeded to form 91% and 67% OH exposed polymer after 10 h and 8h, respectively. SEC analysis revealed the polymers remained intact following acetal hydrolysis.

Block copolymers by sequential ROCOP. To demonstrate the potential of the ROCOP of **1** to produce a diversity of copolymers incorporating more complex architecture, including block copolymers (*e.g.* with hard-soft or orthogonally reactive blocks), sequential addition ROCOP experiments were performed (Scheme 2).

Scheme 2. Block copolymers by sequential ROCOP.

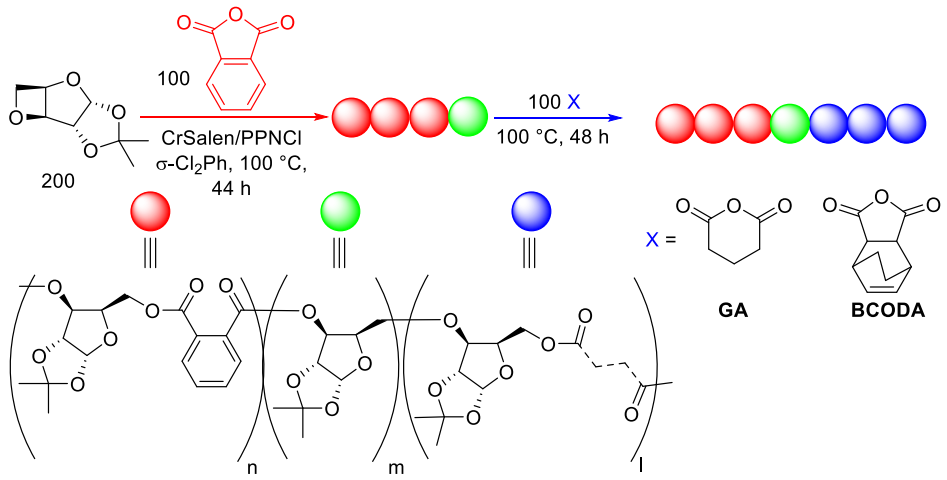

Reactions were carried out at 100 °C in σ-dichlorobenzene with [**1**]$_0$:[**PA**]$_0$:[**CrSalen**]$_0$:[PPNCl]$_0$ loadings of 200:100:1:1 and monitored by ^{1}H NMR spectroscopy and SEC. At 50% conversion of **1, GA** was added to the reaction mixture to yield poly(**PA**-*alt*-**1**-*b*-**GA**-*alt*-**1**). An increase in molar mass was observed upon addition of the second batch of

anhydride ($M_{n,SEC}$ before **GA** addition = 7000 g mol^{-1}, $Đ_M$ = 1.50, $M_{n,SEC}$ after **GA** addition = 8800 g mol^{-1}, $Đ_M$ = 1.36, Figure S172). ^{1}H DOSY NMR spectroscopy of isolated poly(**PA**-*alt*-**1**-*b*-**GA**-*alt*-1). revealed that resonances associated with **PA**, **GA** and **1** shared a single diffusion coefficient (1.89 x 10^{-6} s^{-1}, Figure S109) consistent with the incorporation of all three species within the same polymer chains. Another sequential addition experiment was also performed with **BCODA** under otherwise analogous conditions, to give poly(**PA**-*alt*-**1**-*b*-**BCODA**-*alt*-**1**) ($M_{n,SEC}$ before **BCODA** addition = 5900 g mol^{-1}, $Đ_M$ = 1.60, $M_{n,SEC}$ after **GA** addition = 9200 g mol^{-1}, $Đ_M$ = 1.25, Figure S173) as confirmed by ^{1}H DOSY NMR spectroscopy (diffusion coefficient 5.11 x 10^{-6} s^{-}1, Figure S114). As anticipated, ^{1}H and ^{13}C{^{1}H} NMR spectroscopy revealed that the alkene moiety was intact following polymerization (Figure S110 and S111, respectively). For both block co-polymers, limited ether linkages were detected: the **PA**-*alt*-**1**:ether: **GA**-alt-**1** or **BCODA**-*alt*-**1** (n:m:l) ratio was determined by ^{1}H NMR spectroscopy as 76:1:23 and 72:2:26 for poly(**PA**-*alt*-**1**-*b*-**GA**-*alt*-**1**) and poly(**PA**-*alt*-**1**-*b*-**BCODA**-*alt*-**1**), respectively. Moreover, ^{13}C{^{1}H} NMR spectroscopic analysis also revealed that the regioregularity of **PA**/**1** carbonyl resonances was conserved following addition of the second anhydride (Figures S106 and S111, respectively), suggesting limited transesterification reactions and consistent with the formation of well-defined blocks. However, DSC analysis showed that both poly(**PA**-*alt*-**1**-*b*-**GA**-*alt*-1) and poly(**PA**-*alt*-**1**-*b*-**BCODA**-*alt*-**1**) exhibited only a single T_g (110 °C and 148 °C, Figure S147 and S148, respectively), suggesting that there is no microphase separation between the **PA**/**1** and **GA**/**1** or **BCODA**/**1** components. This is likely as a result of relatively short block lengths in both cases.

CONCLUSION

In summary, ROCOP of a D-xylose-based oxetane with cyclic anhydrides has been used to synthesize an array of sugar-based polyesters, with up to 100% renewable content. The polyesters were shown to exhibit increased thermal stability ($T_{d,onset}$ 212–296 °C) compared with previously reported xylose-based polycarbonates, with a broad range of T_gs accessible (60–145 °C). By exploiting the living character of the ROCOP process, block copolymer synthesis was also possible through sequential co-monomer addition experiments. The impact on thermal properties of exposing the OH groups of the sugar moiety was studied in detail, revealing a significant loss in thermal stability compared with 1,2-acetal protected analogues. The xylose hydroxy groups could be reacted further, and phosphorylation was demonstrated. The internal alkene of some of the anhydride moieties can also be subject to thiol-ene reactions. Combining those orthogonal strategies affords AB co-polyesters with alternating functional substituents. Future work will focus on the development of higher molar mass polymers through the development of bespoke, more active ROCOP catalysts, the exploration of stereochemical enhancement of polymer properties and the application of highly functionalized polymers for self-assembly.

AUTHOR INFORMATION

Corresponding Author

* Antoine Buchard, email: a.buchard@bath.ac.uk

Author Contributions

The manuscript was written through contributions of all authors. All authors have given approval to the final version of the manuscript.

Funding Sources

The Royal Society (RG/150538, UF/160021 fellowship to AB, RGF\R1\180036 studentship to EFC). The UK EPSRC (studentship for TMG).

Notes

The authors declare no competing financial interests.

ACKNOWLEDGMENT

Analytical facilities were provided through the Material and Chemical Characterisation Facility (MC^2) at the University of Bath. We thank the University of Bath HPC for computing resources, the UK EPSRC and the University of Bath (studentship for TMG), as well as the Royal Society (RG/150538, UF/160021 fellowship to AB, RGF\R1\180036 studentship to EFC) for research funding. Prof. Charlotte K Williams and Gregory S. Sulley are thanked for the provision of the dinuclear catalysts and for useful discussions when preparing the manuscript.

ASSOCIATED CONTENT

Supporting Information. Experimental and computational procedures; processed NMR spectra of monomer and polymers and associated digital repository with primary NMR spectroscopic data; plots of M_n and $Đ_M$ *vs*. conversion, polymerization kinetic data, images of SEC traces, MALDI-ToF MS, TGA-MS, DSC traces and WAXS profiles; DFT calculations data and associated digital repository (PDF).

REFERENCES

(1) Bozell, J. J.; Petersen, G. R. Technology development for the production of biobased products from biorefinery carbohydrates—the US Department of Energy's "Top 10" revisited. *Green Chem.* **2010,** *12* (4), 539-554.

(2) Fenouillot, F.; Alain, R.; Colomines, G.; Saint Loup, R.; Pascault, J.-P. Polymers from renewable 1,4:3,6-dianhydrohexitols (isosorbide, isomannide and isoidide): A review. *Prog. Polym. Sci.* **2010**, 578-622.

(3) Galbis, J. A.; de Gracia García-Martín, M.; Violante de Paz, M.; Galbis, E. Synthetic Polymers from Sugar-Based Monomers. *Chem. Rev.* **2016,** *116* (3), 1600-1636.

(4) Gregory, G. L.; López-Vidal, E. M.; Buchard, A. Polymers from sugars: cyclic monomer synthesis, ring-opening polymerisation, material properties and applications. *Chem. Commun.* **2017,** *53* (14), 2198-2217.

(5) Xiao, R.; Grinstaff, M. W. Chemical synthesis of polysaccharides and polysaccharide mimetics. *Prog. Polym. Sci.* **2017,** *74*, 78-116.

(6) Felder, S. E.; Redding, M. J.; Noel, A.; Grayson, S. M.; Wooley, K. L. Organocatalyzed ROP of a Glucopyranoside Derived Five-Membered Cyclic Carbonate. *Macromolecules* **2018,** *51* (5), 1787-1797.

(7) Lonnecker, A. T.; Lim, Y. H.; Wooley, K. L. Functional Polycarbonate of a D-Glucal-Derived Bicyclic Carbonate via Organocatalytic Ring-Opening Polymerization. *ACS Macro Lett.* **2017,** *6* (7), 748-753.

(8) Mikami, K.; Lonnecker, A. T.; Gustafson, T. P.; Zinnel, N. F.; Pai, P.-J.; Russell, D. H.; Wooley, K. L. Polycarbonates Derived from Glucose via an Organocatalytic Approach. *J. Am. Chem. Soc.* **2013,** *135* (18), 6826-6829.

(9) Shen, Y. Q.; Chen, X. H.; Gross, R. A. Polycarbonates from sugars: Ring-opening polymerization of 1,2-O-isopropylidene-D-xylofuranose-3,5-cyclic carbonate (IPXTC). *Macromolecules* **1999,** *32* (8), 2799-2802.

(10) Gregory, G. L.; Jenisch, L. M.; Charles, B.; Kociok-Köhn, G.; Buchard, A. Polymers from Sugars and CO_2: Synthesis and Polymerization of a D-Mannose-Based Cyclic Carbonate. *Macromolecules* **2016,** *49* (19), 7165-7169.

(11) Hibert, G.; Grau, E.; Pintori, D.; Lecommandoux, S.; Cramail, H. ADMET polymerization of α,ω-unsaturated glycolipids: synthesis and physico-chemical properties of the resulting polymers. *Polym. Chem.* **2017,** *8* (24), 3731-3739.

(12) Piccini, M.; Leak, D. J.; Chuck, C. J.; Buchard, A. Polymers from sugars and unsaturated fatty acids: ADMET polymerisation of monomers derived from D-xylose, D-mannose and castor oil. *Polym. Chem.* **2020,** *11* (15), 2681-2691.

(13) Gregory, G. L.; Kociok-Köhn, G.; Buchard, A. Polymers from sugars and CO_2: ring-opening polymerisation and copolymerisation of cyclic carbonates derived from 2-deoxy- D-ribose. *Polym. Chem.* **2017,** *8* (13), 2093-2104.

(14) Tsao, Y.-Y. T.; Wooley, K. L. Synthetic, Functional Thymidine-Derived Polydeoxyribonucleotide Analogues from a Six-Membered Cyclic Phosphoester. *J. Am. Chem. Soc.* **2017,** *139* (15), 5467-5473.

(15) López-Vidal, E. M.; Gregory, G. L.; Kociok-Köhn, G.; Buchard, A. Polymers from sugars and CS_2: synthesis and ring-opening polymerisation of sulfur-containing monomers derived from 2-deoxy-d-ribose and d-xylose. *Polym. Chem.* **2018,** *9* (13), 1577-1582.

(16) Song, Y.; Ji, X.; Dong, M.; Li, R.; Lin, Y.-N.; Wang, H.; Wooley, K. L. Advancing the Development of Highly-Functionalizable Glucose-Based Polycarbonates by Tuning of the Glass Transition Temperature. *Journal of the American Chemical Society* **2018,** *140* (47), 16053-16057.

(17) Longo, J. M.; Sanford, M. J.; Coates, G. W. Ring-Opening Copolymerization of Epoxides and Cyclic Anhydrides with Discrete Metal Complexes: Structure–Property Relationships. *Chem. Rev.* **2016,** *116* (24), 15167-15197.

(18) Paul, S.; Zhu, Y.; Romain, C.; Brooks, R.; Saini, P. K.; Williams, C. K. Ring-opening copolymerization (ROCOP): synthesis and properties of polyesters and polycarbonates. *Chem. Commun.* **2015,** *51* (30), 6459-6479.

(19) Kember, M. R.; Buchard, A.; Williams, C. K. Catalysts for CO_2/epoxide copolymerisation. *Chem. Commun.* **2011,** *47* (1), 141-163.

(20) Luo, M.; Li, Y.; Zhang, Y. Y.; Zhang, X. H. Using carbon dioxide and its sulfur analogues as monomers in polymer synthesis. *Polymer* **2016,** *82*, 406-431.

(21) Abel, B. A.; Lidston, C. A. L.; Coates, G. W. Mechanism-Inspired Design of Bifunctional Catalysts for the Alternating Ring-Opening Copolymerization of Epoxides and Cyclic Anhydrides. *J. Am. Chem. Soc.* **2019,** *141* (32), 12760-12769.

(22) Lidston, C. A. L.; Abel, B. A.; Coates, G. W. Bifunctional Catalysis Prevents Inhibition in Reversible-Deactivation Ring-Opening Copolymerizations of Epoxides and Cyclic Anhydrides. *J. Am. Chem. Soc.* **2020,** *142* (47), 20161-20169.

(23) Su, Y.-C.; Ko, B.-T. Alternating Copolymerization of Carbon Dioxide with Epoxides Using Highly Active Dinuclear Nickel Complexes: Catalysis and Kinetics. *Inorg. Chem.* **2021,** *60* (2), 852-865.

(24) Huang, L.-S.; Tsai, C.-Y.; Chuang, H.-J.; Ko, B.-T. Copolymerization of Carbon Dioxide with Epoxides Catalyzed by Structurally Well-Characterized Dinickel Bis(benzotriazole iminophenolate) Complexes: Influence of Carboxylate Ligands on the Catalytic Performance. *Inorg. Chem.* **2017,** *56* (11), 6141-6151.

(25) Sulley, G. S.; Gregory, G. L.; Chen, T. T. D.; Peña Carrodeguas, L.; Trott, G.; Santmarti, A.; Lee, K.-Y.; Terrill, N. J.; Williams, C. K. Switchable Catalysis Improves the Properties of CO_2-Derived Polymers: Poly(cyclohexene carbonate-*b*-ε-decalactone-*b*-cyclohexene carbonate) Adhesives, Elastomers, and Toughened Plastics. *J. Am. Chem. Soc.* **2020,** *142* (9), 4367-4378.

(26) Gregory, G. L.; Sulley, G. S.; Carrodeguas, L. P.; Chen, T. T. D.; Santmarti, A.; Terrill, N. J.; Lee, K.-Y.; Williams, C. K. Triblock polyester thermoplastic elastomers with semi-aromatic polymer end blocks by ring-opening copolymerization. *Chem. Sci.* **2020,** *11* (25), 6567-6581.

(27) Chen, T. T. D.; Carrodeguas, L. P.; Sulley, G. S.; Gregory, G. L.; Williams, C. K. Bio-based and Degradable Block Polyester Pressure-Sensitive Adhesives. *Angew. Chem. Int. Ed.* **2020,** *59* (52), 23450-23455.

(28) Ahmad, S.; Yousaf, M.; Mansha, A.; Rasool, N.; Zahoor, A. F.; Hafeez, F.; Rizvi, S. M. A. Ring-opening reactions of oxetanes: A review of methodology development and synthetic applications. *Synth. Commun.* **2016,** *46* (17), 1397-1416.

(29) Bull, J. A.; Croft, R. A.; Davis, O. A.; Doran, R.; Morgan, K. F. Oxetanes: Recent Advances in Synthesis, Reactivity, and Medicinal Chemistry. *Chem. Rev.* **2016,** *116* (19), 12150-12233.

(30) Baba, A.; Kashiwagi, H.; Matsuda, H. Reaction of carbon dioxide with oxetane catalyzed by organotin halide complexes: control of reaction by ligands. *Organometallics* **1987,** *6* (1), 137-140.

(31) Baba, A.; Meishou, H.; Matsuda, H. Copolymerisation of oxetane with carbon-dioxide with organotin halide Lewis base systems. *Makromol. Chem. Rapid Commun.* **1984,** *5* (10), 665-668.

(32) Darensbourg, D. J.; Ganguly, P.; Choi, W. Metal Salen Derivatives as Catalysts for the Alternating Copolymerization of Oxetanes and Carbon Dioxide To Afford Polycarbonates. *Inorg. Chem.* **2006,** *45* (10), 3831-3833.

(33) Darensbourg, D. J.; Horn Jr, A.; Moncada, A. I. A facile catalytic synthesis of trimethylene carbonate from trimethylene oxide and carbon dioxide. *Green Chem.* **2010,** *12* (8), 1376-1379.

(34) Darensbourg, D. J.; Moncada, A. I. Tuning the Selectivity of the Oxetane and CO_2 Coupling Process Catalyzed by (Salen)CrCl/n-Bu_4NX: Cyclic Carbonate Formation vs Aliphatic Polycarbonate Production. *Macromolecules* **2010,** *43* (14), 5996-6003.

(35) Darensbourg, D. J.; Moncada, A. I. (Salen)Co(II)/n-Bu_4NX Catalysts for the Coupling of CO_2 and Oxetane: Selectivity for Cyclic Carbonate Formation in the Production of Poly-(trimethylene carbonate). *Macromolecules* **2009,** *42* (12), 4063-4070.

(36) Darensbourg, D. J.; Moncada, A. I.; Choi, W.; Reibenspies, J. H. Mechanistic Studies of the Copolymerization Reaction of Oxetane and Carbon Dioxide to Provide Aliphatic Polycarbonates Catalyzed by (Salen)CrX Complexes. *J. Am. Chem. Soc.* **2008,** *130* (20), 6523-6533.

(37) Darensbourg, D. J.; Moncada, A. I.; Wei, S.-H. Aliphatic Polycarbonates Produced from the Coupling of Carbon Dioxide and Oxetanes and Their Depolymerization via Cyclic Carbonate Formation. *Macromolecules* **2011,** *44* (8), 2568-2576.

(38) Fujiwara, M.; Baba, A.; Matsuda, H. The cycloaddition of heterocumulenes to oxetanes in the presence of catalytic amounts of tetraphenylstibonium iodide. *J. Heterocycl. Chem.* **1989,** *26* (6), 1659-1663.

(39) Takeuchi, D.; Aida, T.; Endo, T. The first example of the copolymerization of cyclic acid anhydrides with oxetane by bulky titanium bisphenolates. *Macromol. Rapid Commun.* **1999,** *20* (12), 646-649.

(40) Kameyama, A.; Ueda, K.; Kudo, H.; Nishikubo, T. The First Synthesis of Alternating Copolymers of Oxetanes with Cyclic Carboxylic Anhydrides Using Quaternary Onium Salts. *Macromolecules* **2002,** *35* (10), 3792-3794.

(41) Buchard, A.; McGuire, T. M.; Bowles, J.; Deane, E.; Farrar, E. H. E.; Grayson, M. N. Control of Crystallinity and Stereocomplexation of Synthetic Carbohydrate Polymers from D- and L-Xylose. *Angew. Chem. Int. Ed.* **2021,** *60*, 4524-4528.

(42) Chen, X.; Gross, R. A. Versatile Copolymers from [L]-Lactide and [D]-Xylofuranose. *Macromolecules* **1999,** *32* (2), 308-314.

(43) Shen, Y.; Chen, X.; Gross, R. A. Aliphatic Polycarbonates with Controlled Quantities of d-Xylofuranose in the Main Chain. *Macromolecules* **1999,** *32* (12), 3891-3897.

(44) Uryu, T. Y., Koyama, Y. Matsuzaki, K. Selective ring-opening polymerization of 3,5-anhydro-1,2-O-isopropylidene-α-D-xylofuranose: Synthesis of [3-5]-D-xylan *Makromol. Chem.* **1984,** *185* (10), 2099-2107.

(45) Uryu, T. Y., Koyama, Y. Matsuzaki, K. Cationic, Ring-Opening Polymerization of 3,5-anhydro-1,2-*O*--isopropylidene-α-D-xylofuranose. *J. Polym. Sci. Polym. Lett. Ed.* **1979,** *17*, 673-678.

(46) Huijser, S.; HosseiniNejad, E.; Sablong, R.; de Jong, C.; Koning, C. E.; Duchateau, R. Ring-Opening Co- and Terpolymerization of an Alicyclic Oxirane with Carboxylic Acid Anhydrides and CO_2 in the Presence of Chromium Porphyrinato and Salen Catalysts. *Macromolecules* **2011,** *44* (5), 1132-1139.

(47) DiCiccio, A. M.; Coates, G. W. Ring-Opening Copolymerization of Maleic Anhydride with Epoxides: A Chain-Growth Approach to Unsaturated Polyesters. *J. Am. Chem. Soc.* **2011,** *133* (28), 10724-10727.

(48) Darensbourg, D. J.; Poland, R. R.; Escobedo, C. Kinetic Studies of the Alternating Copolymerization of Cyclic Acid Anhydrides and Epoxides, and the Terpolymerization of Cyclic Acid Anhydrides, Epoxides, and CO_2 Catalyzed by (salen)$Cr^{III}Cl$. *Macromolecules* **2012,** *45* (5), 2242-2248.

(49) Romain, C.; Garden, J. A.; Trott, G.; Buchard, A.; White, A. J. P.; Williams, C. K. Di-Zinc–Aryl Complexes: CO_2 Insertions and Applications in Polymerisation Catalysis. *Chem. Eur. J.* **2017,** *23* (30), 7367-7376.

(50) Chen, T. T. D.; Zhu, Y.; Williams, C. K. Pentablock Copolymer from Tetracomponent Monomer Mixture Using a Switchable Dizinc Catalyst. *Macromolecules* **2018,** *51* (14), 5346-5351.

(51) Zhu, Y.; Romain, C.; Williams, C. K. Selective Polymerization Catalysis: Controlling the Metal Chain End Group to Prepare Block Copolyesters. *J. Am. Chem. Soc.* **2015,** *137* (38), 12179-12182.

(52) Spyros, A.; Argyropoulos, D. S.; Marchessault, R. H. A Study of Poly(hydroxyalkanoate)s by Quantitative ^{31}P NMR Spectroscopy: Molecular Weight and Chain Cleavage. *Macromolecules* **1997,** *30* (2), 327-329.

(53) Winkler, M.; Romain, C.; Meier, M. A. R.; Williams, C. K. Renewable polycarbonates and polyesters from 1,4-cyclohexadiene. *Green Chem.* **2015,** *17* (1), 300-306.

(54) Hosseini Nejad, E.; van Melis, C. G. W.; Vermeer, T. J.; Koning, C. E.; Duchateau, R. Alternating Ring-Opening Polymerization of Cyclohexene Oxide and Anhydrides: Effect of Catalyst, Cocatalyst, and Anhydride Structure. *Macromolecules* **2012,** *45* (4), 1770-1776.

(55) Aida, T.; Inoue, S. Metalloporphyrins as Initiators for Living and Immortal Polymerizations. *Acc. Chem. Res.* **1996,** *29* (1), 39-48.

(56) van Meerendonk, W. J.; Duchateau, R.; Koning, C. E.; Gruter, G.-J. M. Unexpected side reactions and chain transfer for zinc-catalyzed copolymerization of cyclohexene oxide and carbon dioxide. *Macromolecules* **2005,** *38* (17), 7306-7313.

(57) Hauenstein, O.; Reiter, M.; Agarwal, S.; Rieger, B.; Greiner, A. Bio-based polycarbonate from limonene oxide and CO_2 with high molecular weight, excellent thermal resistance, hardness and transparency. *Green Chem.* **2016,** *18* (3), 760-770.

(58) Van Zee, N. J.; Sanford, M. J.; Coates, G. W. Electronic Effects of Aluminum Complexes in the Copolymerization of Propylene Oxide with Tricyclic Anhydrides: Access to Well-Defined, Functionalizable Aliphatic Polyesters. *J. Am. Chem. Soc.* **2016,** *138* (8), 2755-2761.

(59) Fieser, M. E.; Sanford, M. J.; Mitchell, L. A.; Dunbar, C. R.; Mandal, M.; Van Zee, N. J.; Urness, D. M.; Cramer, C. J.; Coates, G. W.; Tolman, W. B. Mechanistic Insights into the Alternating Copolymerization of Epoxides and Cyclic Anhydrides Using a (Salph)AlCl and Iminium Salt Catalytic System. *J. Am. Chem. Soc.* **2017,** *139* (42), 15222-15231.

(60) Van Zee, N. J.; Coates, G. W. Alternating Copolymerization of Propylene Oxide with Biorenewable Terpene-Based Cyclic Anhydrides: A Sustainable Route to Aliphatic Polyesters with High Glass Transition Temperatures. *Angew. Chem. Int. Ed.* **2015,** *54* (9), 2665-2668.

(61) Wan, Z.-Q.; Longo, J. M.; Liang, L.-X.; Chen, H.-Y.; Hou, G.-J.; Yang, S.; Zhang, W.-P.; Coates, G. W.; Lu, X.-B. Comprehensive Understanding of Polyester Stereocomplexation. *J. Am. Chem. Soc.* **2019,** *141* (37), 14780-14787.

(62) Stößer, T.; Sulley, G. S.; Gregory, G. L.; Williams, C. K. Easy access to oxygenated block polymers via switchable catalysis. *Nat. Commun.* **2019,** *10*, 9.

(63) Gregory, G. L.; Hierons, E. M.; Kociok-Köhn, G.; Sharma, R. I.; Buchard, A. CO_2-Driven stereochemical inversion of sugars to create thymidine-based polycarbonates by ring-opening polymerisation. *Polym. Chem.* **2017,** *8* (10), 1714-1721.

(64) Sanford, M. J.; Peña Carrodeguas, L.; Van Zee, N. J.; Kleij, A. W.; Coates, G. W. Alternating Copolymerization of Propylene Oxide and Cyclohexene Oxide with Tricyclic Anhydrides: Access to Partially Renewable Aliphatic Polyesters with High Glass Transition Temperatures. *Macromolecules* **2016,** *49* (17), 6394-6400.

(65) Peña Carrodeguas, L.; Martín, C.; Kleij, A. W. Semiaromatic Polyesters Derived from Renewable Terpene Oxides with High Glass Transitions. *Macromolecules* **2017,** *50* (14), 5337-5345.

(66) Yi, N.; Chen, T. T. D.; Unruangsri, J.; Zhu, Y.; Williams, C. K. Orthogonal functionalization of alternating polyesters: selective patterning of $(AB)_n$ sequences. *Chem. Sci.* **2019,** *10* (43), 9974-9980.